Macromolecules

ARTICLE

pubs.acs.org/Macromolecules

Synthesis and Photovoltaic Properties of New Low Bandgap Isoindigo-Based Conjugated Polymers

Guobing Zhang,[†] Yingying Fu,[‡] Zhiyuan Xie,*[,‡] and Qing Zhang*[,†]

[†]Department of Polymer Science and Engineering, School of Chemistry and Chemical Engineering, Shanghai Jiao Tong University, Shanghai 200240, China

[‡]State Key Laboratory of Polymer Physics and Chemistry, Changchun Institute of Applied Chemistry, Chinese Academy of Science, Changchun 130022, China

Supporting Information

ABSTRACT: A series of new isoindigo-based low banbap polymers, containing thiophene, thieno[3,2-*b*]thiophene and benzo[1,2-*b*:4,5-*b*′]dithiophene as donors, have been synthesized by Stille cross-coupling reaction. Their photophysical, electrochemical and photovoltaic properties have been investigated. These new polymers exhibit broad and strong absorption between 400 and 800 nm with absorption maxima around 700 nm. The HOMO energy levels of polymers vary between −5.20 and −5.49 eV and the LUMO energy levels range from −3.66 to −3.91 eV. The optical bandgaps of the polymers are optimized for solar cell applications and they are at about 1.5 eV. Polymer solar cells (PSC) based on these new polymers were fabricated with device structures of ITO/PEDOT:PSS/polymers: $PC_{71}BM$ (1:2, w/w)/LiF/Al. The photovoltaic properties of the polymers have been evaluated under AM 1.5G illumination at 100 mW/cm^2 with a solar simulator. The combination of broad absorption, optimal bandgap and well matched energy levels with those of PCBMs makes these isoindigo-based low bandbap polymers promising materials for photovoltaic applications.

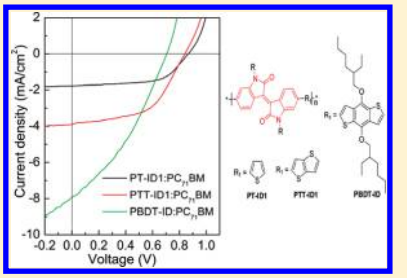

INTRODUCTION

Organic photovoltaic (OPV) with many advantages such as low cost, lightweight, and solution processability may become an important part of renewable energy in the future.[1] Low band gap conjugated polymers have attracted considerable attention recently because of their applications in organic solar cell devices. Bulk-heterojunction (BHJ) based on blending of electron-donating conjugated polymers and high-electron-affinity fullerene derivatives such as PCBMs is the most successful device structure for polymer solar cell so far.[2] Many new conjugated polymers have been synthesized for high performance OPV applications.[3] The design rules for donor polymers in fullerene based BHJ devices are low HOMO energy level for high open circuit voltage, low band gap for large solar photon harvest, balanced crystallinity and solubility for high hole mobility and for optimal morphology, and well-matched HOMO/LUMO energy levels between polymers and those of fullerenes for efficient charge separation.[4] Development of new monomers may lead to synthesis of interesting polymers with tailor-made photophysical, electrochemical and other properties to fulfill those requirements for high performance solar cells.

(*E*)-1*H*,1′*H*-[3,3′]biindolylidene-2,2′-dione (isoindigo) which can be obtained from various natural sources is one of the indigoid natural organic dyes.[5] Its derivatives are active constituents in some traditional Chinese medicine and have recently emerged as a promising scaffold for antileukemia activities.[6] Unlike blue-colored indigo, isoindigo itself is brown colored and has absorption maxima at 365 and 490 nm in dimethyl sulfoxide solution. Isoindigo also shows better stability than indigo when expose to light.[5] Crystallographic study on alkyl substituted isoindigo shows that the central carbon−carbon double bond has an *E* configuration and is conjugated with two indole heterocycles to form perfect planar π-conjugated structure.[7] Recently, there are some successful examples of introduction high performance dyes into conjugated polymers and oligomers.[3c,8] Polymers based on electron deficient diketopyrrolopyrrole (DPP) dye as acceptors have achieved power conversion efficiencies (PCEs) of 5.5%.[9] Isoindigo, which contains two lactam rings, is another electron-deficient dye. The perfect planar π-conjugated structure and a strong electron-withdrawing effect make it ideal monomer for synthesis of donor/acceptor low bandgap conjugated polymer for organic solar cell applications. Isoindigo-based oligothiophenes and polymers have been reported by Reynolds and co-workers.[10] The isoindigo-based oligomers showed interesting absorption spectra and low HOMO energy levels.[10a] Here, we present the synthesis of five new low bandgap polymers based on isoindigo (**ID**) units and different electron-donors (thiophene, thieno[3,2-*b*]thiophene and benzo[1,2-*b*:4,5-*b*′]-dithiophene), and the characterization of their thermal, optical, electrochemical, and photovoltaic properties.

Received: October 15, 2010
Revised: January 13, 2011
Published: February 04, 2011

Scheme 1. Synthesis of Monomers

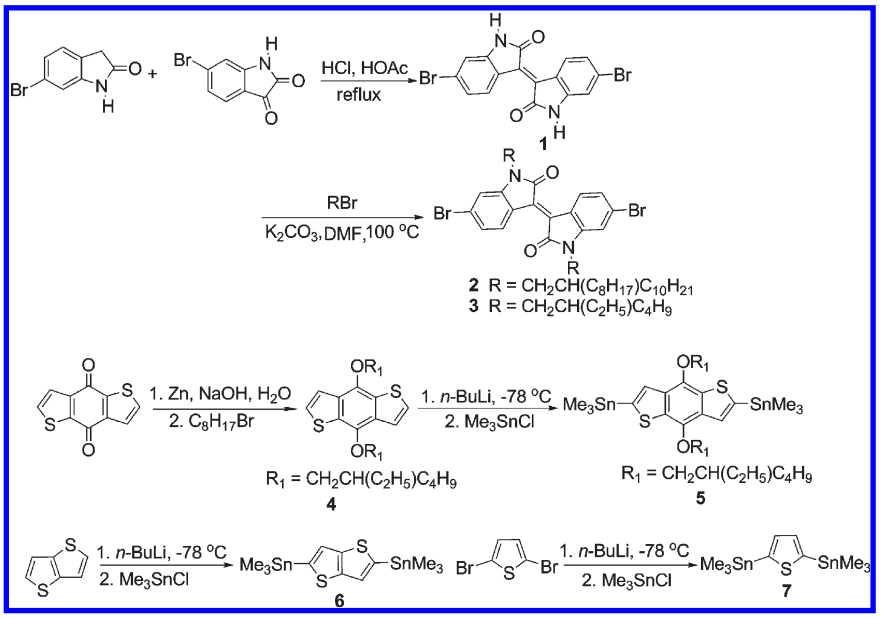

Scheme 2. Synthesis of Isoindigo-Based Polymers

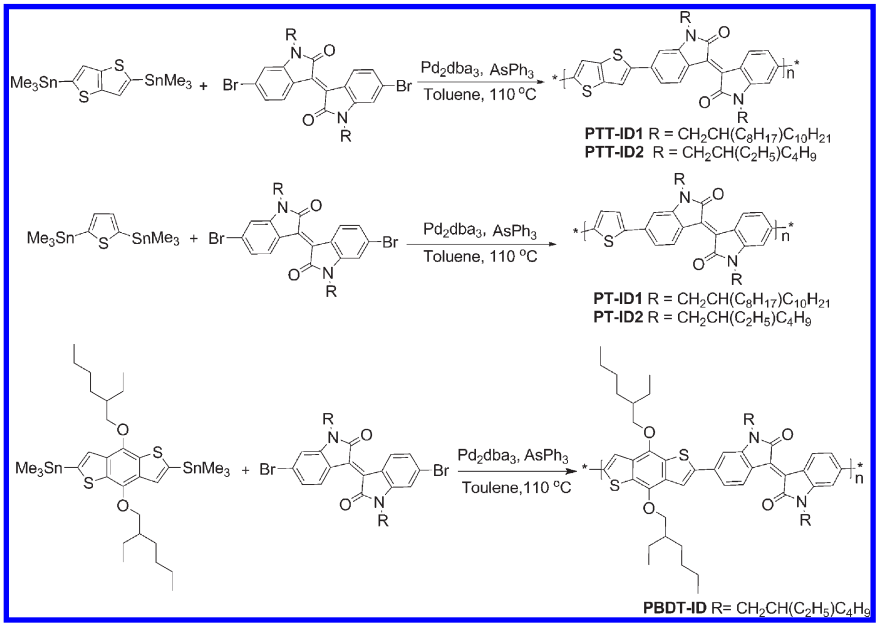

RESULTS AND DISCUSSION

Synthesis and Characterization of Polymers. The synthetic routes for monomers and polymers were illustrated in Scheme 1 and 2. The commercially available 6-bromoisatin and 6-bromooxindole were refluxed in acetic acid and hydrochloric acid under nitrogen to give a brown solid 6,6′-dibromoisoindigo (**1**) in 77.6% yield.[10] Because of the strong $\pi-\pi$ interactions and hydrogen bonding, the brown solid is only slightly soluble in common organic solvents. To improve the solubility of isoindigo monomer, branched 2-octyldodecyl and 2-ethylhexyl side chains were attached to both lactam nitrogen atoms. The alkylated 6,6′-dibromoisoindigo monomers **2** and **3** was obtained in 64.2% and 48.9% yield, respectively. The tin monomers **5**, **6**, and **7** were prepared according to the literature methods.[11] The polymers were synthesized by Stille cross-coupling reactions with 1:1 monomer ratio in presence of tris(dibenzylideneacetone)-dipalladium ($Pd_2(dba)_3$) as catalyst and triphenylarsine as ligand to give purple-blue materials. The crude polymer was purified by precipitating in methanol and washing with methanol and hexane in a Soxhlet extractor for 24 h each. The residue was extracted with hot chloroform or chlorobenzene in an extractor for 24 h. Polymer **PT-ID1**, **PTT-ID1**, and **PBDT-ID** are soluble and can be extracted with hot chloroform or chlorobenzene. After removing solvent, purple-blue solids were collected. Polymer **PT-ID2** and **PTT-ID2** with 2-ethylhexyl side chains were

dx.doi.org/10.1021/ma102357b |*Macromolecules* 2011, 44, 1414–1420

Table 1. Molecular Weights and Thermal Properties of Polymers

polymer	yield (%)	M_n[a] (kDa)	M_w[a] (kDa)	PDI[a]	T_d (°C)[b]
PT-ID1	69.2	17.2	36.1	2.1	397
PTT-ID1	72.3	37.6	127.8	3.4	397
PBDT-ID	76.6	21.9	32.6	1.5	348

[a] M_n, M_w, and PDI of polymers were determined by GPC using polystyrene standards with THF as eluent. [b] The temperature of 5% weight-loss under nitrogen.

insoluble in any solvent. The large branched side chains or multiple short branched side chains are required to ensure the solubility of isoindigo based polymers. The chemical structures of the polymer **PT-ID1**, **PTT-ID1**, and **PBDT-ID** were verified by ^{1}H NMR spectroscopy. The spectra were included in Supporting Information. These three polymers showed good solubility in solvents such as chloroform and chlorobenzene. The number-average molecular weights (M_n) and polydispersity indexes of the polymers were determined by gel permeation chromatography (GPC) using polystyrenes as standards with tetrahydrofuran as eluent. GPC data are listed in Table1. The reported number-average molecular weights (M_n) were measured at room temperature. They may not accurately reflect average molecular weight of single polymer chain when there is strong intermolecular interaction and polymer aggregation.

Thermal Stability. Thermogravimetric analyses of polymers were displayed in the Table 1 and Figure S1 in the Supporting Information. The temperature of 5% weight-loss was chose as onset point of decomposition (T_d). Polymer **PT-ID1**, **PTT-ID2**, and **PBDT-ID** were thermally stable up to 397, 397, and 348 °C. Thermal properties of polymers are important for device application. The new polymers showed good thermal stability for application in PSCs and other optoelectronic devices. Neither polymers displayed noticeable glass transition in differential scanning calorimetry (DSC) analysis.

Optical Properties. The optical properties of polymers were also analyzed. The UV−vis absorption spectra of the polymers in chloroform solution and as thin films are shown in Figure 1. The optical properties of the polymers were summarized in Table 2. Polymer **PT-ID1** showed two absorption bands in chloroform solution. The first absorption band maximum at 466 nm is relatively weak compared to isoindigo-based oligothiophenes,[10a] and the second absorption band of **PT-ID1** is broad and red-shifted (λ_{max}^{abs} at 684 nm) compared to isoindigo-based oligomer (λ_{max}^{abs} at 579 and 560 nm,). The red-shifted absorption of the polymer **PT-ID1** is expected because of increasing effective conjugation in polymer. However, the relatively weak absorption of polymer in short wavelength (400−530 nm) compared to oligomers need further study. The **PTT-ID1** polymer with thieno[3,2-*b*]thiophene as donor showed similar optical properties but its absorption spectrum was further red-shift (λ_{max} at 717 nm). Polymer **PBDT-ID** showed almost the same absorption spectra as **PT-ID1** in the range of 500−800 nm. All the three polymers exhibited shoulder peaks in the visible region. The film absorption spectra of polymers were depicted in Figure 1b. The absorption maxima of **PT-ID1**, **PTT-ID1**, and **PBDT-ID** solid films were at 694, 718, and 688 nm, respectively. The absorption spectra of polymer films showed little change compared to their solution absorption spectra. The branched side chains may have adverse effect on the intermolecular interaction of polymers and prevent effective intermolecular stacking. The edges of the film

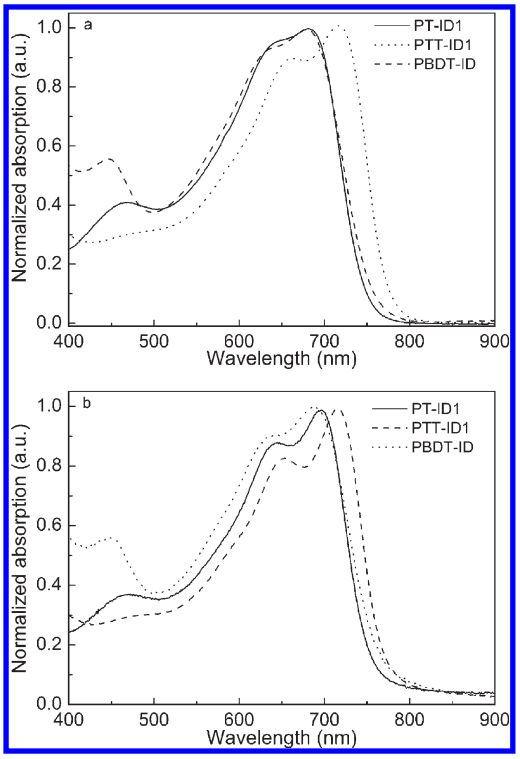

Figure 1. Normalized UV−vis spectra of isoindigo-based polymers (a) in chloroform solution and (b) as thin film.

absorption bands for **PT-ID1**, **PTT-ID1**, and **PBDT-ID** were at 786, 800, and 803 nm, respectively. The optical bandgaps (E_g^{opt}) were calculated from the absorption edges of solid state films. The optical bandgaps of **PT-ID1**, **PTT-ID1**, and **PBDT-ID** were 1.58, 1.55, and 1.54 eV, respectively. The absorption spectra of polymer films showed good overlap with solar flux at sea level, which has a maximum at about 700 nm.

Electrochemical Properties. The electrochemical properties of polymers were investigated by cyclic voltammetry (CV). The cyclic voltammograms of **PT-ID1**, **PTT-ID1**, and **PBDT-ID** films are shown in Figure 2. The potentials were referenced to the ferrocene/ferrocenium redox couple (Fc/Fc^+). The redox potential of Fc/Fc^+ was assumed an absolute energy level of −4.8 eV to vacuum.[12] The redox potential of Fc/Fc^+ was measured under the same condition as polymer sample and was located at 0.09 V related to the Ag/Ag^+ electrode. The CV data were summarized in Table 2. The onset oxidation potentials of **PT-ID1**, **PTT-ID1**, and **PBDT-ID** were located at 0.78, 0.72, and 0.49 eV respectively. The HOMO energy levels of the polymers were calculated according to the equation: HOMO = $-(E_{onset}^{ox} + 4.71)$ eV. The HOMO energy levels of polymers are shown in Table 2. The HOMO energy level of **PT-ID1** was the lowest at −5.49 eV, the HOMO energy level of **PTT-ID1** was at −5.43 eV, and the HOMO energy level of **PBDT-ID** was the highest at −5.20 eV among three isoindigo-based polymers. The relatively lower HOMO energy levels of these isoindigo-based polymers can be attributed to electron deficient lactam rings in isoindigo repeating units. The LUMO energy levels of **PT-ID1**, **PTT-ID1**, and **PBDT-ID** were −3.91, −3.88, and −3.66 eV calculated from the optical band gaps and HOMO energy levels of the polymers. These new polymers possess relatively low HOMO energy level for high open circuit voltage and suitable LUMO energy level for charge separation, together with low

Table 2. Optical and Redox Properties of Polymers

	solution λ (nm)	film λ (nm)			oxidation (V, vs Ag/Ag^+ in CH_3CN)			
polymer	λ_{max}^{abs}	λ_{max}^{abs}	λ_{onset}^{abs}	E_g^{opt} (eV)[a]	E_{onset}^{ox} (V)	HOMO (eV)[b]	E_{onset}^{red} (V)[c]	LUMO (eV)[d]
PT-ID1	684	694	786	1.58	0.78	−5.49	−0.80	−3.91
PTT-ID1	717	718	800	1.55	0.72	−5.43	−0.83	−3.88
PBDT-ID	680	688	803	1.54	0.49	−5.20	−1.05	−3.66

[a] Calculated from UV absorption spectrum of polymer film by the equation: band gap =1240/λ_{onset}^{abs}. [b] HOMO = −(4.71 + E_{onset}^{ox}). [c] $E_{onset}^{red} = E_{onset}^{ox} - E_g^{opt}$. [d] LUMO = E_g^{opt} + HOMO.

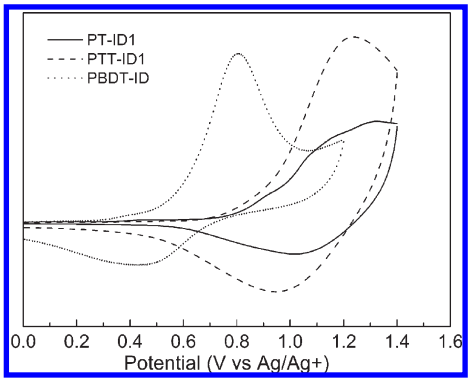

Figure 2. Cyclic voltammograms of isoindigo-based polymers thin films.

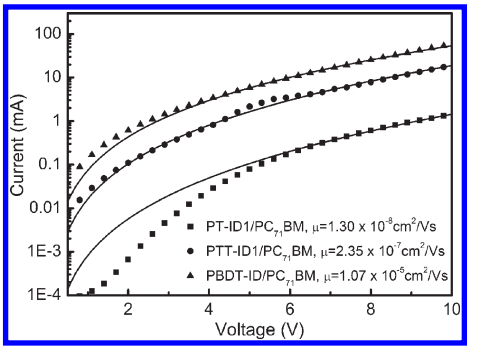

Figure 3. Charge-carrier mobilities of polymer/$PC_{71}BM$ (1:2) blend films.

optical band gaps for large solar photon harvest. On the basis of the systematic study and comprehensive consideration, ideal polymer for OPV application was proposed before.[13] It might have a LUMO energy level of about −3.9 eV (0.3 eV higher than those of PCBMs), a HOMO energy level of about −5.4 eV, and a bandgap of about 1.5 eV for optimal performance. In many aspects, these newly synthesized polymers closely resemble the ideal low band gap polymers suggested by Scharber, Brabec, and others in design rules of polymers for organic solar cell applications.[13b,14]

Charge Transport in Polymer/$PC_{71}BM$ Blends. Hole-only devices were fabricated with the configuration of ITO/PEDOT:PSS/polymer (or polymer:$PC_{71}BM$)/MoO_3/Al. The hole mobilities were measured by space charge limited current (SCLC) method and were calculated by following equation:

$$J = \frac{9}{8}\varepsilon\varepsilon_0\mu \exp\left(\gamma\sqrt{\frac{V}{L}}\right)\frac{V^2}{L^3}$$

where J is the current density, V is the applied voltage, L is the thickness of the active layer, μ is the mobility, ε is the dielectric constant, ε_0 is the permittivity of free space, and γ is the field-activation factor.

Figure 3 showed the relationship between current and voltage in the hole-only devices of polymer/$PC_{71}BM$ (1:2) blend films. The calculated hole mobilities of **PT-ID1**/$PC_{71}BM$, **PTT-ID1**/$PC_{71}BM$ and **PBDT-ID**/$PC_{71}BM$ blend films were 1.30×10^{-8}, 2.35×10^{-7}, and 1.07×10^{-5} $cm^2/(V\,s)$, respectively. The hole mobilities of polymers were much lower than electron mobilities of PCBMs ($\sim 10^{-3}$ $cm^2/(V\,s)$). The mismatch of charge mobilities might be the key reason that limited the performance of solar cell devices.

Photovoltaic Properties. Polymer solar cell devices with polymer **PT-ID1**, **PTT-ID1**, and **PBDT-ID** as electron donors and $PC_{71}BM$ as electron acceptor were fabricated. The device structure was ITO/PEDOT:PSS/polymer:$PC_{71}BM$/LiF/Al. Solar cell devices were characterized under AM 1.5G illumination at 100 mW/cm^2 with a solar simulator. The photovoltaic performances of the devices with different polymer/$PC_{71}BM$ weight ratio were summarized in Table 3. The polymer/$PC_{71}BM$ weight ratio of 1:2 showed the best device performance. Figure 4 displayed the current−voltage curves of the devices and corresponding values of open-circuit voltage (V_{oc}), short circuit currents (J_{sc}), fill factors (FF), and power conversion efficiencies (PCE). At 1:2 weight ratio of polymer/$PC_{71}BM$, the device with **PT-ID**/$PC_{71}BM$ as active layer (70 nm) gave a V_{oc} value of 0.87 V, a FF of 60%, and a J_{sc} value of 1.76 mA/cm^2, resulted a PCE value of 0.92%. The devices with **PTT-ID**/$PC_{71}BM$ as active layer (65 nm) showed a V_{oc} of 0.84 V, a J_{sc} of 3.90 mA/cm^2, and a FF of 53%, resulted a PCE of 1.74%. The devices with **PBDT-ID**/$PC_{71}BM$ as active layer (80 nm) exhibited a V_{oc} of 0.71 V, a J_{sc} of 7.93 mA/cm^2, a FF of 34%, and a PCE of 1.91%. The polymer **PTT-ID** containing device demonstrated a better photovoltaic performance than the polymer **PT-ID** containing device. The better performance of polymer **PTT-ID** than polymer **PT-ID** may be attributed to the combined factors such absorption, molecular weights and hole mobility. The open-circuit voltages were related to the HOMO energy levels of polymers. The polymer **PT-ID1** had the lowest HOMO energy level and the OPV device containing this polymer had the highest V_{oc}. The large branched side chains effectively improved the solubility of the polymers. However, they might also greatly reduce the crystallinty of polymer, thereby, resulted in low hole mobility and low J_{sc}. The **PBDT-ID** possessed short branched side chains and the devices showed a J_{sc} value as high as 7.93 mA/cm^2. It was significantly higher than that of **PT-ID1** and **PTT-ID1** containing devices. The AFM imagines also showed that the

Table 3. Photovoltaic Performances of PCS devices

polymer	polymer:$PC_{71}BM$ (w/w)	d (nm)	V_{oc} (V)	J_{sc} (mA/cm^2)	FF (%)	PCE (%)
PT-ID1	1:1	80	0.83	1.68	38	0.53
	1:2	70	0.87	1.76	60	0.92
	1:3	80	0.86	1.69	58	0.85
PTT-ID2	1:1	65	0.84	3.89	43	1.42
	1:2	65	0.84	3.90	53	1.74
	1:3	75	0.85	2.99	51	1.30
PBDT-ID	1:1	85	0.70	5.00	33	1.17
	1:2	80	0.71	7.93	34	1.91
	1:3	90	0.71	7.13	35	1.76

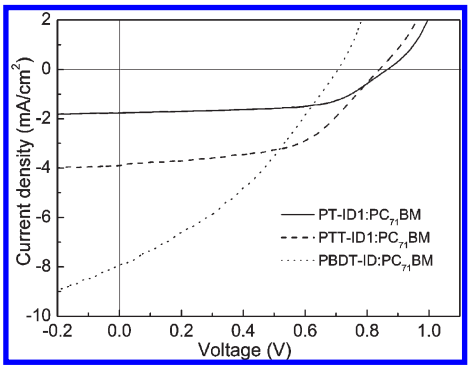

Figure 4. Current−voltage characteristics of solar cell devices under illumination of AM 1.5 G, 100 mW/cm^2.

film of **PBDT-ID**/$PC_{71}BM$ exhibited fine domains compared to the film of **PTT-ID2**/$PC_{71}BM$ (Supporting Information, Figure S4). The external quantum efficiency (EQE) curves of PSC devices were shown in Figure S2 (Supporting Information). The EQE measurements showed that the isoindigo-based devices exhibited very broad photoresponse range from 300 to 800 nm. **PBDT-ID**:$PC_{71}BM$ composite has higher EQE values compared to **PT-ID1**:$PC_{71}BM$ and **PTT-ID1**:$PC_{71}BM$. The EQE value of **PBDT-ID**:$PC_{71}BM$ composite reached 30−40% in the range 350−630 nm. This contributed to the high J_{sc} value.

The moderate performance of isoindigo-based polymer solar cell devices might be attributed to low hole motility of the polymers. They were much lower than the electron mobilities of PCBMs. The unbalanced charge carrier mobility limited the performance of polymer solar cell devices. Optimizations on structures, molecular weights of polymers and morphologies of composites for the improvement of hole mobility are in progress.

CONCLUSIONS

Isoindigo-based conjugated polymers with three different donors have been synthesized. Isoindigo-based conjugated polymers possess relatively low HOMO energy level for high open circuit voltage, a suitable LUMO energy level for charge separation, and optimized optical band gap for polymer solar cell applications. Isoindigo with its perfect planar π-conjugated structure and electron deficient nature can be a useful new monomer for construction of low band gap conjugated polymers. Relative large branched side chains or multiple short branched side chains are required to ensure the solubility of isoindigo based polymers. Preliminary investigations on organic solar cell devices with polymers as donors and $PC_{71}BM$ as acceptor were also carried out. The moderate performance of isoindigo-based polymer solar cell devices might result from unbalanced charge carrier mobility in polymer/PCBM composite. Optimizations on structures, molecular weights of polymer and morphologies of composites for the improvement of hole mobility might result balanced charge carrier mobility in active layer and further enhance the performance OPV devices.

EXPERIMENTAL SECTION

Instrumentation. Nuclear magnetic resonance (NMR) spectra were recorded on a Mercury plus 400 MHz machine. Gel permeation chromatography (GPC) measurements were performed on a Waters 1515 series GPC coupled with UV−vis detector using tetrahydrofuran as eluent with polystyrenes as standards. Thermogravimetric analyses (TGA) were conducted with a TA Instruments QS000IR at a heating rate of 20 °C min^{-1} under nitrogen gas flow. Differential scanning calorimetry (DSC) analysis was performed on a TA Instruments Q2000 in a nitrogen atmosphere. All the samples (about 10.0 mg in weight) were heated up to 300 °C first and held for 2 min to remove thermal history, followed by cooling at the rate of 20 °C/min to 20 °C and then by heating at rate of 20 °C/min to 300 °C. UV−vis absorption spectra were recorded on a Perkin-Elmer model λ 20 UV−vis spectrophotometer. Electrochemical measurements were conducted on a CHI 600 electrochemical analyzer under nitrogen in a deoxygenated anhydrous acetonitrile solution of tetra-*n*-butylammonium hexafluorophosphate (0.1 M). A platinum electrode was used as a working electrode, a platinum-wire was used as an auxiliary electrode, and an Ag/Ag$^+$ electrode was used as a reference electrode. Thin film of polymer was coated on the surface of platinum electrode and ferrocene was chosen as a reference. The atomic force microscope (AFM) measurements were performed on a SPA300HV instrument with a SPI3800 controller (Seiko Instruments).

Device Fabrication and Characterization. Polymer solar cells (PSCs) with the device structures of ITO/PEDOT:PSS/polymer:$PC_{71}BM$/LiF/Al were fabricated as follows: a ca. 40 nm-thick PEDOT:PSS (Baytron P AI 4083) layer was spin-coated from an aqueous solution onto the precleaned ITO substrates. The coated substrates were dried at 120 °C for 30 min in air and were transferred into a nitrogen filled glovebox. A film was spin-coated on top of the PEDOT/PSS layer from a solution containing a mixture of polymer:$PC_{71}BM$ (1:2 weight ratio) in chlorobenzene. The samples were transferred into an evaporator and 1 nm-thick of LiF layer and 100 nm-thick of Al layer with area of 0.12 cm^2 were thermally deposited under a vacuum of 10^{-6} Torr. The devices were encapsulated in a glovebox and were measured in air. Current−voltage characteristics were measured using a computer controlled Keithley 236 source meter. The photocurrents were measured under AM 1.5G illumination at 100 mW/cm^2 from a solar simulator (Oriel, 91160A-1000). Devices for space-charge-limited current

(SCLC) measurements were fabricated in a manner similar to the solar cell devices with the structures of ITO/PEDOT:PSS/polymer: $PC_{71}BM$(1:2)/MoO_3(10 nm)/Al.

Materials. 6-Bromoisatin and 6-bromooxindole were obtained from Darui Chemical Co. Ltd., Shanghai, China. Other materials used in this work were purchased from Sigma-Aldrich Chemical Co., Alfa Aesar Chemical Company and Sinopharm Chemical Reagent Co. Ltd., China. Tetrahydrofuran (THF) and toluene were freshly distilled over sodium wire under nitrogen prior to use.

Synthesis of Monomers and Polymers. The synthetic routes for monomers and polymers are shown in Scheme 1 and Scheme 2. 1-Bromo-2-octyldodecane was synthesized according to the literature methods.[15] Compound **4** and **5** were synthesized in our previous work.[11a]

6,6′-Dibromodi(2-octyldodecyl)isoindigo (2). 6,6′-Dibromoisoindigo (2.0 g, 4.76 mmol) and potassium carbonate (3.3 g, 23.8 mmol) were added to the solution of 1-bromo-2-octyldodecane (4.3 g, 11.9 mmol) in dimethylformamide (60 mL). The mixture was reacted at 100 °C for 18 h, and then was cooled to room temperature. Water (100 mL) was added and the mixture was extracted with dichloromethane. The combined organic layer was dried with anhydrous sodium sulfate. Solvent was removed under reduced pressure and residue was purified by flash chromatography on silica gel with diethyl ether/hexane (1: 30) as eluent to give a deep red solid (3.0 g, 64.2%). ^{1}H NMR ($CDCl_3$, 400 MHz, δ): 9.07 (d, J = 8.8 Hz, 2H), 7.16 (m, 2H), 6.89 (d, J = 1.5 Hz, 2H), 3.62 (d, J = 8.0 Hz, 4H), 1.82−1.94 (s, 2H), 1.20−1.40 (m, 64H), 0.83−0.90 (m, 12H). ^{13}C NMR ($CDCl_3$, 100 MHz, δ): 168.30, 146.41, 132.76, 131.24, 126.87, 125.30, 120.59, 111.74, 44.90, 36.30, 32.13, 32.08, 31.72, 30.20, 29.86, 29.84, 29.81, 29.76, 29.55, 29.50, 26.58, 22.91, 22.88, 14.32.

Polymer PTT-ID1. Tris(dibenzylideneacetone)dipalladium (0.015 g, 0.016 mmol) and triphenylarsine (0.019 g, 0.064 mmol) were added to a solution of compound **2** (0.78 g, 0.79 mmol) and compound **6** (0.37 g, 0.79 mmol) in toluene (20 mL) under nitrogen. The solution was subjected to three cycles of evacuation and admission of nitrogen. The mixture was heated to 110 °C for 48 h. After cooled to room temperature, the mixture was poured into methanol (100 mL) and was stirred for 2 h. A purple-blue precipitate was collected by filtration. The product was purified by washing with methanol and hexane in a Soxhlet extractor for 24 h each. It was extracted with hot chloroform in an extractor for 24 h. After removing solvent, a purple-blue solid was collected (0.55 g, 72.3%). ^{1}H NMR ($CDCl_3$, 400 MHz, δ): 8.2−9.2 (br, 2H), 6.0−7.3 (br, 6H), 3.5−3.8 (br, 4H), 1.96−2.04 (br, 2H), 1.0−1.86 (br, 64H), 0.72−0.94 (br, 12H). M_n = 37.6 kDa, PDI = 3.4.

Polymer PT-ID1. The same procedure was used as for polymer **PTT-ID1**. Compounds used were tris(dibenzylideneacetone)dipalladium (0.013 g, 0.014 mmol), triphenylarsine (0.018 g, 0.056 mmol), compound **2** (0.71 g, 0.72 mmol), and compound **7** (0.30 g, 0.72 mmol). After work-up, a purple-blue solid was obtained (0.45 g, 69.2%). ^{1}H NMR ($CDCl_2CDCl_2$), 400 MHz, δ): 9.0−9.1 (br, 2H), 6.58−7.50 (br, 6H), 3.50−3.80 (br, 4H), 1.80−2.0 (br, 2H), 1.15−1.50 (br, 64H), 0.80−0.95 (br, 12H). M_n = 17.2 kDa, PDI = 2.1.

Polymer PBDT-ID. The same procedure was used as for polymer **PTT-ID1**. Compounds used were tris(dibenzylideneacetone)dipalladium (0.015 g, 0.016 mmol), triphenylarsine (0.020 g, 0.064 mmol), compound **3** (0.52 g, 0.80 mmol), and compound **5** (0.62 g, 0.80 mmol). It was extracted with hot chlorobenzene in an extractor for 24 h. After removing solvent, a purple-blue solid was obtained (0.57 g, 76.6%). ^{1}H NMR ($CDCl_3$ and $CDCl_2CDCl_2$, 400 MHz, δ): 8.5−9.3 (br, 2H), 6.0−7.5 (br, 6H), 3.0−4.5 (br, 8H), 0.5−2.2 (br, 60H). M_n = 21.9 kDa, PDI = 1.5.

Polymer PTT-ID2. The same procedure was used as for polymer **PTT-ID1**. Compounds used were tris(dibenzylideneacetone)dipalladium (0.015 g, 0.016 mmol), triphenylarsine (0.020 g, 0.064 mmol), compound **3** (0.52 g, 0.80 mmol), compound **6** (0.37 g, 0.80 mmol), and toluene (30 mL). The polymer was precipitated after heating at 110 °C for 5 h. The precipitate was insoluble in any solvent.

Polymer PT-ID2. The same procedure was used as for polymer **PTT-ID1**. Compounds used were tris(dibenzylideneacetone)dipalladium (0.026 g, 0.029 mmol), triphenylarsine (0.035 g, 0.115 mmol), compound **3** (0.93 g, 1.44 mmol), compound **7** (0.59 g, 1.44 mmol), and toluene (40 mL). The polymer was precipitated after heating at 110 °C for 5 h. The precipitate was insoluble in any solvent.

■ ASSOCIATED CONTENT

Supporting Information. Text giving experimental section, characterization, materials, and instrumentation and figures showing TGA curves, EQE curves, AFM images, and NMR spectra. This material is available free of charge via the Internet at http://pubs.acs.org.

■ AUTHOR INFORMATION

Corresponding Authors
*E-mail: qz14@sjtu.edu.cn (Q.Z.); xiezy_n@ciac.jl.cn (Z.Y.X.).

■ ACKNOWLEDGMENT

This work was supported by National Nature Science Foundation of China (NSFC Grant Nos. 20674049 and 20834005) and Shanghai municipal government (Grant Nos. B202 and 10ZZ15).

■ REFERENCES

(1) (a) Brabec, C. J.; Sariciftci, N. S.; Hummelen, J. C. *Adv. Funct Mater.* **2001**, *11*, 15. (b) Kim, J. Y.; Lee, K.; Coates, N. E.; Moses, D.; Nguyen, T. Q.; Dante, M.; Heeger, A. J. *Science* **2007**, *317*, 222. (c) Peet, J.; Kim, J. Y.; Coates, N. E.; Ma, W. L.; Moses, D.; Heeger, A. J.; Bazan, G. C. *Nat. Mater.* **2007**, *6*, 497. (d) Hou, J.; Chen, H.-Y.; Zhang, S.; Li, G.; Yang, Y. *J. Am. Chem. Soc.* **2008**, *130*, 16144. (e) Ahmed, E.; Kim, F. S.; Xin, H.; Jenekhe, S. A. *Macromolecules* **2009**, *42*, 8615. (f) Chen, H.-Y.; Hou, J.; Zhang, S.; Liang, Y.; Yang, G.; Yang, Y.; Yu, L.; Wu, Y.; Li, G. *Nat. Photo.* **2009**, *3*, 649. (g) Huo, L.; Hou, J.; Zhang, S.; Chen, H.-Y.; Yang, Y. *Angew. Chem.* **2010**, *122*, 1542. (h) Park, S. H.; Roy, A.; Beaupre, S.; Cho, S.; Coates, N.; Moon, J. S.; Moses, D.; Leclerc, M.; Lee, K.; Heeger, A. J. *Nat. Photo.* **2009**, *3*, 297.

(2) (a) Yu, G.; Gao, J.; Hummelen, J. C.; Wudl, F. A.; Heeger, A. J. *Science* **1995**, *270*, 1789. (b) Coakley, K.; Mcgehee, M. D. *Chem. Mater.* **2004**, *16*, 4533.

(3) (a) Dennler, C.; Scharber, M. C.; Brabec, C. J. *Adv. Mater.* **2009**, *21*, 1323. (b) He, Y.; Chen, H. Y.; Hou, J.; Li, Y. *J. Am. Chem. Soc.* **2010**, *132*, 1377. (c) Huo, L.; Hou, J.; Chen, H.-Y.; Zhang, S. J.; Jiang, Y.; Chen, T. L.; Yang, Y. *Macromolecules* **2009**, *42*, 6564. (d) Zhao, G.; He, Y.; Li, Y. *Adv. Mater.* **2010**, *22*, 4355.

(4) (a) Blouin, N.; Michaud, A.; Gendron, D.; Wakim, S.; Blair, E.; Neagu-Plesu, R.; Belletete, M.; Durocher, G.; Tao, Y.; Leclerc, M. *J. Am. Chem. Soc.* **2008**, *130*, 732. (b) Scharber, M. C.; Muhlbacher, D.; Koppe, M.; Denk, P.; Waldauf, C.; Heeger, A. J.; Brabec, C. J. *Adv. Mater.* **2006**, *18*, 789. (c) Bredas, J.-L.; Beljonne, D.; Coropceanu, V.; Cornil, J. *Chem. Rev.* **2004**, *104*, 4971.

(5) Puchalska, M.; Połec-Pawlak, K.; Zadrozna, I.; Hryszko, H.; Jarosz, M. *J. Mass Spectrom.* **2004**, *39*, 1441.

(6) Weea, X. K.; Yeo, W. K.; Zhang, B.; Tan, V. B. C.; Lim, K. M.; Tay, T. E.; Go, M. *Bioorg. Med. Chem.* **2009**, *17*, 7562.

(7) Yuan, M.; Fang, Q.; Ji, L.; Yu, W. *Acta Crystallogr.* **2007**, *E63*, o4342.

(8) (a) Zou, Y.; Gendron, D.; Badrou-Aıch, R.; Najari, A.; Tao, Y.; Leclerc, M. *Macromolecules* **2009**, *42*, 2891. (b) Tamayo, A. B.; Tantiwiwat, M.; Walker, B.; Nguyen, T.-Q. *J. Phys. Chem. C* **2008**, *112*, 15543. (c) Burgi, L.; Turbiez, M.; Pfeiffer, R.; Bienewald, F.; Kirner, H.-J.; Winnewisser, C. *Adv. Mater.* **2008**, *20*, 2217. (d) Zou, Y.; Gendron, D.; Neagu-Plesu, R.; Leclerc, M. *Macromolecules* **2009**, *42*, 6361. (e) Wienk, M. M.; Turbiez, M.; Gilot, J.; Janssen, R. A. J. *Adv. Mater.* **2008**, *20*, 2556.

(9) Bijleveld, J. C.; Gevaerts, V. S.; Di Nuzzo, D.; Turbiez, M.; Mathijssen, S. G. J.; de Leeuw, D. M.; Wienk, M. M.; Janssen, R. A. J. *Adv. Mater.* **2010**, *22*, E242.

(10) (a) Mei, J.; Graham, K. R.; Stalder, R.; Reynolds, J. R. *Org. Lett.* **2010**, *12*, 660. (b) Stalder, R.; Mei, J.; Reynolds, J. R. *Macromolecules* **2010**, *43*, 8348.

(11) (a) Zhang, G.; Fu, Y.; Xie, Z.; Zhang, Q. *Chem. Commun.* **2010**, *46*, 4997. (b) Lee, J.-Y.; Shin, W.-S.; Haw, J.-R.; Moon, D.-K. *J. Mater. Chem.* **2009**, *19*, 4938. (c) Pham, C. V.; Macomber, R. S., Jr; H., B. M.; Zimmer, H. *J. Org. Chem.* **1984**, *49*, 5250.

(12) Li, Y.; Cao, Y.; Gao, J.; Wang, D.; Yu, G.; Heeger, A. J. *Syn. Met.* **1999**, *99*, 243.

(13) (a) Koster, L. J. A.; Mihailetchi, V. D.; BLOM, P. W. M. *Appl. Phys. Lett.* **2006**, *88*, 093511. (b) Thompson, B. C.; Frechet, J. M. J. *Angew. Chem., Int. Ed.* **2008**, *47*, 58.

(14) Scharber, M. C.; Muhlbacher, D.; Koppe, M.; Denk, P.; Waldauf, C.; Heeger, A. J.; Brabec, C. J. *Adv. Mater.* **2006**, *18*, 789.

(15) Jones, L.; Schumm, J. S.; Tour, J. M. *J. Org. Chem.* **1997**, *62*, 1388.